

## INVESTIGATION OF DEPOSITS FORMATION IN STEAM SUPERHEATERS DURING COMBUSTION OF HALLOYSITE DOPED BIOMASS

Sylwester Kalisz<sup>1\*</sup>, Waldemar Gądek<sup>1</sup>, Joanna Wnorowska<sup>1</sup>, Izabella Maj<sup>1</sup>, Szymon Ciukaj<sup>1</sup>, Piotr Płaza<sup>2</sup>, Alexander Mack<sup>2</sup>, Jörg Maier<sup>2</sup>

<sup>1</sup>Silesian University of Technology, Institute of Power Engineering and Turbomachinery  
Konarskiego 20, 44-100 Gliwice, Poland

\*corresponding author: Sylwester.Kalisz@polsl.pl

<sup>2</sup>Stuttgart University, Institute of Combustion and Power Plant Technology  
Pfaffenwaldring 23, 70569 Stuttgart, Germany

**ABSTRACT:** This paper presents the results from the experimental investigation of the impacts of mineral additive halloysite on reducing slag and corrosive deposits formation, commonly found in boilers fired with K-Cl enriched agricultural biomass. The selected three types of agricultural biomass doped with halloysite and one reference coal were fired under different thermal conditions simulated in two pulverized fuel reactors from University of Stuttgart (USTUTT) and Silesian University of Technology (SUT). During the appropriate tests performed at the reactor furnace temperatures ranged between 1200°C and 900°C, the uncooled and cooled ash deposits and fly ashes were collected to determine their mass, elemental composition and structure (by SEM/EDX analysis) to get better understanding of the additive impacts on deposit formation. Moreover, more fundamental additional tests with different additive/KCl mass ratios were carried out to investigate interactions between halloysite and KCl under varied temperature and residence time conditions. The positive impact of halloysite on the change of deposit structure was confirmed and the halloysite effects on deposit formation rate in a temperature window of 1200°C-900°C were discussed in comparison with the results obtained from the pure biomass and coal combustion tests.

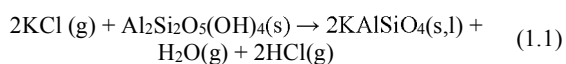
**Keywords:** biomass, combustion, mineral additives, slagging, fouling, ashes

### 1 INTRODUCTION

#### 1.1 Prevention of corrosive ash deposits formation by using additives

In the last decade, co-firing of biomass or/and full conversion of coal fired boilers into biomass firing become, in the light of more strict EU environmental legislation, a realistic scenario for existing coal fired conventional boilers. Although, a CO<sub>2</sub> neutral biomass is regarded as highly beneficial for lowering green gas emissions, its combustion may lead to serious ash-related boiler operational problems. Slagging, fouling and rapid corrosion of the furnace walls and boiler heat exchange surfaces are the main drawbacks associated with firing enriched in potassium and chlorine agricultural biomass.

In order to mitigate the ash related issues during combustion, various countermeasures including fireside additives [1] such as boiler injection of aluminosilicate-based additives or sulfur-based additives (ammonium sulfate or solid sulfur), clean wood co-firing [3], [4] or fuel pre-treatment (e.g. alkalis leaching) [5], [6] have been attempted. Fireside additives are the simplest method to minimize ash slagging and fouling propensity in a boiler as are easily fed to any type of furnace including stocker furnaces, fluidized furnaces or pulverized fuel fired furnaces. Fuel additives refer to a group of chemicals or minerals which can influence on the ash chemistry, decrease the concentration of problematic species or increase the ash melting temperatures. Various aluminosilicate based minerals can be used during combustion to capture easily volatile alkali metals, mainly potassium which is present in relatively high amount in agricultural biomass. This group of mineral additives includes e.g. kaolinite, bentonite, bauxite or halloysite for which the reaction with potassium chloride can be expressed as follows (eq. 1.1).



Chemical binding is claimed to be the most common effect of additives, due to converting problematic ash elements into high-temperature stable substances[2]. However, to achieve good process efficiency with additive use, an excess of additive is required. Therefore, determination of proper additive/fuel ratio is important for the optimization of process conditions and decreasing costs of additive dosage.

Most of fundamental studies of K-capture by solid additives have been carried out in fixed bed or thermogravimetric reactors, where reaction conditions such as residence time, temperature, contact between reagents etc. significantly differ from those applied under pulverized fuel fired conditions. The effect of potassium retention and chlorine liberation was examined in laboratory scale by applying several types of aluminosilicates and fly ash. Three mineral additives: kaolin, bentonite and halloysite appeared to be effective in potassium binding at high temperature melting potassium aluminosilicates and in liberating chlorine in the temperature range of 800°C–1000°C [11].

The results provided by Wang et al. [12] showed that under suspension-fired conditions (1100°C-1450°C), kaolin and coal fly ash can effectively capture gaseous potassium. When increasing the mass ratio of KCl to Al-Si additives in the reactants, the conversion of KCl to K-aluminosilicate decreased. However, when reaction temperature increased from 1100°C to 1450°C, the conversion of KCl does not change significantly, which differs from the trend observed in fixed-bed reactor.

The reaction of kaolin powder with KCl, K<sub>2</sub>CO<sub>3</sub> and K<sub>2</sub>SO<sub>4</sub> under suspension-fired conditions was studied by Wang et al [13]. Research include experiments taking place in entrained flow reactor as well as equilibrium calculations and show a significant K-capture potential of kaolinite. Kaolin and mullite have the potential to capture KOH as well. Wang et al [14] found that the amount of potassium captured by kaolin generally followed the equilibrium at temperatures above 1100°C, but lower conversion was observed at 800°C and 900°C.

Crystalline kaliophillite ( $\text{KAlSiO}_4$ ) was formed at higher temperatures (1300°C and 1450°C), whereas, amorphous K-aluminosilicate was formed at lower temperatures. The experimental tests performed at IFK in down fired pf 500kW furnace with kaolinite and ammonium sulphate as well confirmed the good effectiveness of the used additives in decreasing ash deposition when firing straw [33].

As far as coal fly ash is concerned as additive, it was found that it can reduce the amount of particles rich in K, Cl and S and in general reduce the formation of combustion aerosols during pulverized wood combustion [10]. Injection of fly ash to reduce ash deposition and corrosion problems is also commercially applied in some biomass pf boilers in Denmark.

Regarding the halloysite, some successful trials with halloysite dosage for the ash deposit mitigation have been carried out in a large scale coal fired pf utility boiler in Poland [17]. However, in case of biomass (co-)firing still more fundamental studies are needed to get better understanding of halloysite capability to capture potassium originated from biomass and its impact on ash deposit formation.

## 1.2 The aim of the work

In this work, more fundamental experimental and thermochemical studies were carried out to investigate interactions between iron-rich halloysite and KCl under different additive to KCl ratios and thermal conditions simulated in two types of reactors from Silesian University of Technology (SUT) and University of Stuttgart (USTUTT). The main aim was to investigate the impacts of the additive dosage on potassium capture by additive and KCl conversion to prevent salts condensation and formation of corrosive ash deposits. In the next part of the experiments, the optimal ratios of additive were selected and mixed with chlorine and alkali rich agricultural biomasses to be fired in both reactors to study the influence of additive on the ash deposit formation during biomass combustion. On the one side, the USTUTT focused on the ash deposits formation at the temperature range of 1100°C-1200°C which corresponds to the thermal conditions of the outer layer of ash deposits formed in superheaters placed at the furnace outlet. On the other side, the SUT investigated deposits formed on the air-cooled stainless steel probe placed at 900°C flue gas temperature and surface temperature of 480°C, under typical normal operation conditions of steam superheaters in pulverized fuel fired boilers.

## 2 MATERIALS AND METHODS

### 2.1 Additive and KCl

The halloysite used in this study, as Al-Si based mineral additive for biomass enhancement, originated from mine DUNINO located in southwestern Poland. Halloysite is one of the aluminosilicate clay minerals classified to the kaolin sub group with a chemical composition similar to kaolinite. In its fully hydrated form the halloysite formula is  $\text{Al}_2\text{Si}_2\text{O}_5(\text{OH})_4 \cdot 2\text{H}_2\text{O}$ . What differs halloysite from kaolinite  $\text{Al}_2\text{Si}_2\text{O}_5(\text{OH})_4$  is that it contains additional water molecules between the layers. Halloysite is often observed in a partly dehydrated state since it loses its interlayer water molecules easily above 60°C. Its inner specific surface can be ten times bigger than kaolinite [16] and reaches approximately 70–

85 m<sup>2</sup>/g. It is a mineral of low hardness (1–2 in Mohs scale), with around 3000 kg/m<sup>3</sup> density, and high temperature resistance. Halloysite belongs to the group of two-layered minerals but, as opposed to kaolinite, in halloysite the individual packets composed of a layer of silicon tetrahedra and aluminum octahedra are separated from each other, or they form small packets with a thickness much smaller than in the case of kaolinite packets. Halloysite is characterized by the ability of ions absorption both on the outer surface and inside the crystal [16]. Consequently halloysite can be claimed to be a more effective fuel additive than kaolinite. The high reactivity of halloysite is a consequence of a phase change at a temperature above 550 °C, which allows the formation of high melting compounds with alkali metals [16]- [19].

As compared to its pure crystal form the halloysite used in this study was enriched with iron and other impurities with the bulk oxide composition shown in Table I. Volatile content and ash fusion temperatures are shown in Table II and Table III. It was delivered to USTUTT in a powder form (particles with granulation 0-100 µm) with the particle size distribution as shown in Fig. 1.

**Table I:** Major oxide analysis of halloysite.

Oxide	Al <sub>2</sub> O <sub>3</sub>	SiO <sub>2</sub>	Fe <sub>2</sub> O <sub>3</sub>	TiO <sub>2</sub>	P <sub>2</sub> O <sub>5</sub>
Mass fraction, wt.-%	22.7	36.1	16.0	2.18	0.59
Oxide	CaO	K <sub>2</sub> O	Na <sub>2</sub> O	SO <sub>3</sub>	MnO
Mass fraction, wt.-%	0.533	0.17	0.173	0.016	0.261

**Table II:** Volatile content of halloysite.

Volatile analysis	Mass fraction, wt.-%
Moisture (105 °C)	1.73
Crystal water (105 °C - 360 °C)	4.74
Volatiles (360 °C – 910 °C)	9.25

**Table III:** Ash fusion temperature of halloysite.

Ash fusion temperature	Temperature, °C
Initial deformation temperature (IDT)	900
Softening Temperature (ST)	1430
Fluid Temperature (FT)	1460

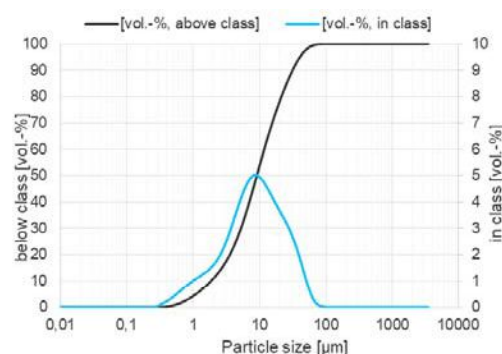


**Figure 1:** Particle size distribution of the used halloysite (USTUTT).

The KCl is one of dominant alkali salts present in agricultural biomass which originates mostly from fertilisers which are added to artificially modify soil in order to provide plants with sufficient quantities of nutrients needed for a vigorous growth and increased yield. Potassium is also naturally present in plants. During biomass combustion, potassium is released to gas phase in different forms depending on the fuel chemistry (S and Cl contents) and combustion conditions and may interact with other ash forming elements, condense and form corrosive deposits in convective part of the boiler's heat exchangers. The presence of KOH, K<sub>2</sub>CO<sub>3</sub>, KCl and K<sub>2</sub>SO<sub>4</sub> has been detected in the ashes from biomass-fired boilers [28]. KCl has a melting point of 770°C but salt eutectics could melt at lower temperatures (about 550°C) and lead to accelerated corrosion and slagging problems. Fireside additives are used to change the ash composition and reduce the existence of volatile alkali species [2], [20]- [22]. For the tests presented in this study, in more detail described in section 3, the following mixtures based on halloysite/KCl mass ratios were prepared [34] : raw halloysite (0% KCl), 2:1, 5:1, 10:1 and 20:1.

## 2.2 Investigated fuels

In this study, three types of biomass (marked as DS0, BS – cereal straw, BZ0 – herbaceous pellets, SPK0, BW – wheat straw) enriched with the halloysite additive and hard coal (marked as WS) from Polish mine KWK Sobieski were investigated. Specified as DS4, BZ2, SPK4, BSA, BWA are fuel samples with halloysite 4.0%, 2.0%, 4.0%, 9.0% and 4.0% by additive mass input,

respectively. Results of the analysis are presented in Table IV. The content of alkali metals (K and Na) and (Al+Si)/(K+Na) ratio have a significant impact on deposit formation tendency. Investigated biomass samples are characterized with a substantial content of alkali metals (from 0.79% to 1.33% wt.) compared to the investigated coal sample (0.65% wt.). Additionally, the biomass samples have lower sulfur content (varied between 0.08 and 0.11% wt.) as compared to the coal (1.46% wt.).

The fuels have been delivered in pelletized form with varying diameters and lengths. In order to perform combustion tests the grain size of the fuel has to be below 500 µm. Therefore, the fuel pellets undergo a milling and sieving process.

Fuel particle size distribution (PSD) is a very important parameter determining sufficient burnout, flame properties and heat exchange in pulverized fuel boiler. In order to determine size distribution, sieve analysis was done by using the vibrating test stand LPZE-2e MULTI SERW with mesh size, as follows: 1000, 500, 355, 250, 125, 90 µm. Particle size distributions of the biomass fuels investigated by SUT are presented in Figure 2. Less than 54.0 % of the coal particles are smaller than 90 µm. Furthermore, less than 86.4 % are smaller than 125 µm. In general, biomass particles are coarser and long-edge compared to the round coal particles. Coarser PSD of fuel samples with halloysite dosage results from the halloysite PSD where 77.2 % of additive particles (HA in Figure 1) are smaller than 250 µm.

**Table IV:** Results of proximate and ultimate analysis of investigated fuels and blends with additive.

Proximate analysis wt% (as received)											
No.	WS	DS0	BZ0	SPK0	DS4*	BZ2*	SPK4*	BS	BSA*	BW	BWA
Moisture	3.9	11.7	9.2	13.6	11.7	9.2	13.6	6.7	6.7	11.1	14.6
Ash	13.8	9.13	3.83	4.73	13.13	5.83	8.73	9.55	16.33	8.43	18.6
Volatiles	34.37	61.11	68.11	63.44	58.03	66.55	60.34	67.2	61.95	64.8	55.3
Fixed Carbon	47.93	18.05	18.86	18.22	17.14	18.42	17.33	16.5	15.04	15.7	11.5
Ultimate analysis wt% (as received)											
C	61.69	38.98	43.34	39.69	37.01	42.34	37.75	40.90	37.20	40.7	32.6
H	4.65	4.85	5.38	5.03	4.6	5.25	4.78	5.43	4.94	4.97	4.24
S	1.46	0.11	0.09	0.08	0.11	0.09	0.07	0.125	0.114	0.109	0.103
N	0.98	0.76	2.68	0.49	0.72	2.62	0.47	0.786	0.715	0.649	0.673
Cl	0.34	0.38	0.08	0.16	0.36	0.08	0.15	0.228	0.207	0.142	0.123
Na**	0.34	0.071	0.027	0.017	0.068	0.026	0.016	0.038	0.042	0.021	0.040
K**	0.31	1.26	0.91	0.77	1.210	0.892	0.739	0.799	0.734	0.734	0.635
O	12.53	32.76	34.47	35.42	31.08	33.68	33.68	36.28	33.82	33.90	29.06
LCV (MJ/kg)	23.77	14.37	16.52	14.99	13.64	16.14	14.26	14.47	13.15	14.58	11.74
(Na+K)**	0.65	1.33	0.94	0.79	1.28	0.92	0.76	0.837	0.776	0.755	0.675
(Al+Si)/(K+Na)**	16.46	3.13	3.35	3.30	5.18	6.24	5.66	2.85	6.01	3.11	8.55
*Theoretical fuel-additive mixture as-received state calculated from individual as-received fuel and additive states;											
**Recalculated from the ash elemental analysis, ash produced at 550°C for biomass fuels.											

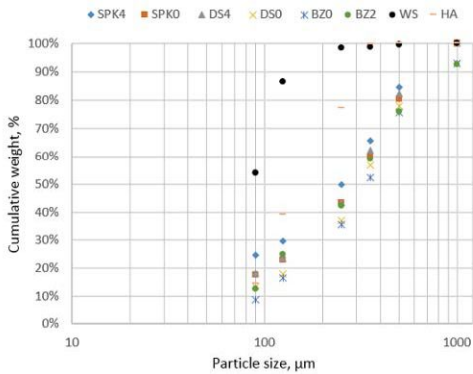


**Figure 2:** Particle size distribution PSD of investigated fuels and raw halloysite (HA).

**2.3 Experimental Facility of SUT**

The Pulverized Fuel-fired vertical Combustion Chamber (PFCC) is an electrically heated stainless steel vertical combustion chamber (30kWth) with a multi-fuel swirl burner and a K-TRON fuel feeder in its upper part. The flue gas outlet and gas cooling system is located at the bottom of the PFCC.

The facility is also equipped with the control and data acquisition system. The reactor is widely used for advanced measurements of pulverized fuel combustion conditions. Scheme of PFCC reactor is presented in Figure 3. For ash deposits formation investigations, a stainless steel deposition probe is used. The probe outer shell temperature is continuously measured by K-type thermocouple and controlled by the Valve Control Unit based on the Siemens Sinamics 7 controller. For probe cooling medium pressurized air is used. An outer diameter of the probe is 37 mm. Mass of deposits are weighed after every test to determine ash collection efficiency CE for every fuel type. Qualitative analysis was carried out on the collected deposits samples including ash oxides analysis, ash fusibility experiments.

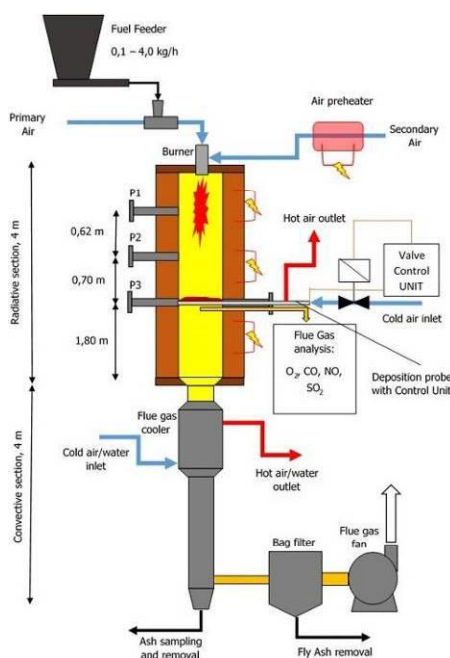


**Figure 3:** Pulverized Fuel Combustion Chamber located in the IPET (SUT).

**2.4 Experimental Facility of USTUT**

Experimental tests were carried out in an atmospheric drop tube furnace – BTS (ger. Brennstofftrennstufung, engl. fuel staging) down-fired vertical reactor. The reactor, as illustrated in Figure 4, consists of an electrically heated ceramic pipe (0.2 m in diameter and a length of 2.5 m) which can be heated up to 1500°C. The maximum electrical input is 22 kW. The pulverized fraction of the fuel is dosed to the burner by a volumetric screw feeder allowing fuel mass flows between 0.2 and 5.0 kg/h, which in case of a hard coal corresponds to 1.5 kW (0.2 kg/h) or 35 kW (5.0 kg/h) fuel power. The combustion atmosphere can be controlled with flow controllers so that different combustion conditions (air, O<sub>2</sub>, CO<sub>2</sub>) can be created. The concentration of the flue gas components O<sub>2</sub>, CO<sub>2</sub>, CO, NO<sub>x</sub> and SO<sub>2</sub> are continuously measured at the end of the combustion chamber, meaning 2.5 m downstream of the fuel injection point. In addition, the HCl concentration in the flue gas is measured with a FTIR analyzer at three different locations with different flue gas temperatures (see Figure 4 (~ 1000°C), B (~ 450°C), C (~ 160°C)). The flue gas components and unburned carbon can be measured and sampled along the reactor center line with a vertically moveable and temperature regulated lance to investigate fuel conversion or solid interactions kinetics. For the ash deposit collection and ash deposition rate measurements a ceramic pipe with 15 mm outer diameter is inserted through the opening at 1.55 m. The mass of deposited ash is recorded as a function of time. More details about the applicability of online deposition sensors to measure and quantify the real time deposition behavior can be found elsewhere [33]. After the experiment, the deposition sample is evaluated in the laboratory.

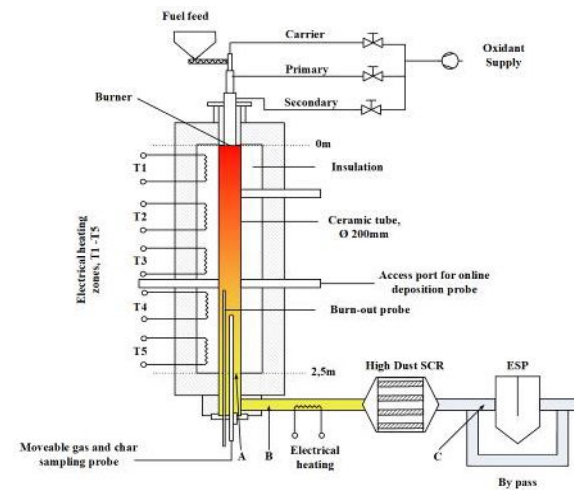


**Figure 4:** BTS pulverized fuel combustion reactor located at IFK (USTUTT).

**2.5 Deposition coefficients and KCl conversion**

In research ash deposition rate and deposition efficiency were used in the order to compare deposit formation of raw biomass and additive doped biomass.

The Deposition Rate DR (g/m<sup>2</sup>min) and CE Collection Efficiency (% kg of deposit/ kg of ash) and of deposit formation were determined as follows [19].

$$DR = \frac{m_{dep}}{F_{probe} \tau} \quad (2.1)$$

where:

$m_{Dep}$  - mass off deposit collected on probe, g

$F_{probe}$  - probe inflow area (deposition area of probe),  $m^2$

$\tau$  - time of probe exposition, min

$$CE = \frac{m_{dep}}{B_{fuel} \left( \frac{A^r}{100} \right) \left( \frac{F_{probe}}{F_{reactor}} \right)} \quad (2.2)$$

where:

$B_{fuel}$  - Fuel stram, kg/h

$A^r$  - ash content of fuel (considering additive stram), % wt.

$F_{reactor}$  - cross section of reactor,  $m^2$

The fuel burnout or unburnt carbon (UBC) in the ash can be expressed in different ways, as a Fixed Carbon (FC) in ash [25], as a UBC in ash [26] or as a Total Organic Carbon (TOC) [27]. In this study, a UBC is used following the equation (3.2) [26], [27]:

$$UBC = \frac{1 - \frac{A^r}{A}}{1 - A^r} \quad (2.3)$$

where:

$A^r$  - fuel ash content, %

$A$  - sample ash content, %

For the KCl/additive ratio experiments performed in the PFCC and BTS reactor, a useful indicator of conversion of potassium chloride ( $KCl_{conv}$ ) was obtained. The indicator presents the degree of KCl conversion via reaction with halloysite. The background of the reaction is that the remaining Cl (not gas released) is forming the KCl, and the potassium that is not soluble in water has been captured with the halloysite. However, some KCl can evaporate into gas phase and react with reactor steel or deposition probe (especially in the case of experiments on PFCC steel reactor).

$$KCl_{conv} = \frac{Cl_{in} - Cl_{probe}}{Cl_{in}} \quad (2.4)$$

where:

$Cl_{in}$  - content of chlorine in inlet KCl/Halloysite mixture, %

$Cl_{probe}$  - content of chlorine in ash deposit collected on deposition probe, or in the fly ash %

**Table V:** Parameters of Additive/KCl tests

Parameter	BTS	PFCC	Unit
	Value	Value	
Reactor temperature	1200	900	$^{\circ}C$
Probe temperature	1200	480	$^{\circ}C$
Time of probe exposition	60	60	min
Mixture halloysite/additive stream	0.25	0.25	kg/h
Total airflow	10.0/8.3	26.0	$m^3/h$
Reactor inner diameter	200	300	mm
Length from burner to deposition probe	1.55	2.2	m
Theoretical gas residence time	4.0-5.0	6.50	s

### 3 RESULTS OF INVESTIGATION

#### 3.1 Results of additive/KCl interactions

In the experiments blends of halloysite and KCl were investigated on the basis of reaction (1.1.), for which a stoichiometric ratio of halloysite/KCl can be calculated, as follows:

$$RATIO = \frac{\text{Molar Mass of halloysite}}{\text{Molar Mass of KCl}} = \frac{258.14 \text{ g/mol}}{74.56 \text{ g/mol}} = 3.46.$$

As an indicator of halloysite/KCl interaction the increased concentration of HCl in the flue gas can be observed and measured by the FTIR analyzer. For the presented experiments, halloysite/KCl ratios were determined by weight. During the tests following mixtures were prepared:

- Raw halloysite (0% KCl)
- Ratio 2:1
- Ratio 5:1
- Ratio 10:1
- Ratio 20:1

The mass ratio of halloysite/KCl=20 corresponds roughly to the case of a mixture of straw with 0.2% chlorine content (as received) and 9.0% of halloysite (see Table I, BSA case).

The halloysite/KCl mixtures were fed via volumetric feeders into the reaction chambers. The experiments were conducted in the ceramic BTS reactor at a flue gas temperature of  $1200^{\circ}C$  with ceramic (not cooled) deposition probes and in the PFCC reactor at a flue gas temperature of  $900^{\circ}C$  with air cooled deposition probes (with probe shell temp.  $480^{\circ}C$  to imitate the real boiler operation condition of the superheaters). Experiments were performed under air conditions in two levels of theoretical gas residence time, for BTS reactor 4.0-5.0s and for PFCC reactor 6.50s. Theoretical gas residence times were calculated using the method presented in reference [27]. The BTS and PFCC reactor operation parameters are shown in Table V. After the experiments, the collected deposits from the deposition probe were weighed and analyzed to determine the chlorine content.

In the next step, the KCl conversion factors were calculated by using formula (2.4) and compared to the preliminary experiments on halloysite/KCl ratios obtained in a small scale muffle furnace at temperatures of 900°C and 1100°C. These tests are widely described in ref. [23]. To achieve more comparable interaction conditions as in pulverized boilers, the test for the same halloysite/KCl ratios were performed in BTS and PFCC reactors at gas temperatures of 900°C, and 1200°C. The results of KCl conversion are presented in the Figure 5.

The highest KCl conversion was obtained in the muffle furnace tests. Even for ratio 2.0 a conversion of 95.7% has been reached. As result of halloysite/KCl interactions, most of the potassium remained in the ash deposits whereas the chlorine was released into the gas phase [23]. For higher ratios, the KCl conversion is practically approaching 100%. When comparing the KCl conversion in the muffle furnace at 900°C and 1100°C temperatures, no significant difference has been observed. In fact, these high KCl conversion results are obtained for long term tests (90 minutes) at constant temperature and thus were promoting conversion in lab conditions far away from practical applications.

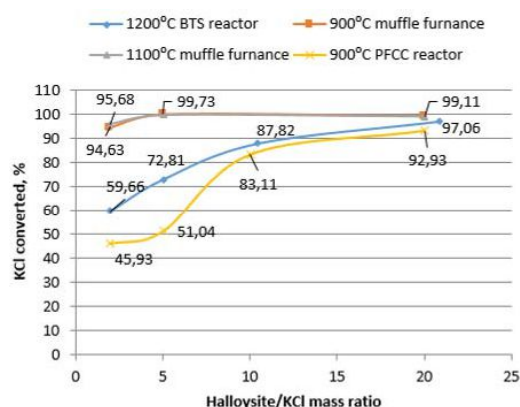


**Figure 5:** KCl converted in different temperature and process conditions.

Results of experiments performed in the BTS and PFCC reactors – reflecting pulverized fuel combustion conditions much closer to industrial reality - show a strong impact of halloysite/KCl ratio on the KCl conversion. For sub-stoichiometric mass ratio 2:1 the 59.66% and 45.93% of KCl conversion is achieved for BTS and PFCC reactor respectively. The highest conversion rate of KCl was obtained for the 20:1 ratio in BTS reactor reaching 97.06% and 92.93% in the PFCC reactor. Considerable different shape of curve for PFCC experiments can be observed and explained by the fact that fraction of KCl (and/or released Cl<sub>2</sub>) reacts with Fe and Cr of reactor steel chamber forming corrosion products under ratio 2:1 and 5:1. Those products are not taken into account when calculating conversion factors.

The experiments performed in BTS reactor revealed the increased concentration of HCl in the flue gas as result of interaction between halloysite and KCl. These findings were also confirmed by the phase equilibrium analysis as described in more detail in ref [23]. The HCl concentrations (in ppm) measured by FTIR analyzer at the furnace outlet of BTS reactor for the halloysite/KCl =20 are shown in Figure 6. The impact of water excess on HCl formation was observed. In case of feeding the pulverized halloysite/KCl mixture in the hot air

atmosphere in BTS without additional water injections, the HCl concentration was of around 9 times lower than with the high water excess. With the additional water injections, the HCl concentration reached max. 211 ppm which was around 60 ppm lower than expected from the theoretical calculations based on the assumption of complete conversion of the released chlorine into HCl.

Similar effect of raising HCl concentration in flue gases was achieved during combustion of biomass with halloysite as shown in Figure 7. However, the measured HCl concentrations were highly depended on the measurement location, and decreased gradually with a temperature drop in the flue gas duct of the BTS reactor. This shows the complexity of possible interactions of HCl with the ash and/or other flue gas components during combustion conditions, which may affect the HCl measurements.

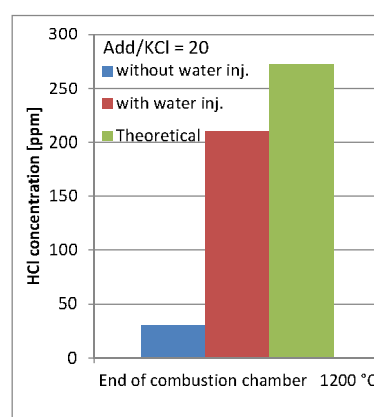


**Figure 6:** Measured and theoretical HCl conc. for halloysite/KCl=20.

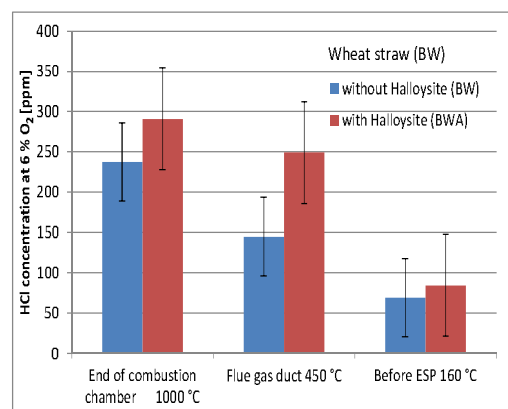


**Figure 7:** Measured HCl con. during combustion of wheat straw with (BWA) and without additive (BW).

### 3.2 Results of ash deposition tendency with additive doped biomass – combustion experiments

In this section, the results obtained from the ash deposition tests conducted at PFCC and BTS reactors are presented and discussed. The main goal was to determine the ash deposition rates and collection efficiencies for halloysite doped biomasses compared with raw biomasses and typical hard coal. The main operation parameters and settings of both combustion reactors during the ash deposition experiments are summarized in Table VI.

**Table VI:** Main PFCC and BTS reactors parameters during and results of the ash deposition tests– combustion of additive doped biomass.

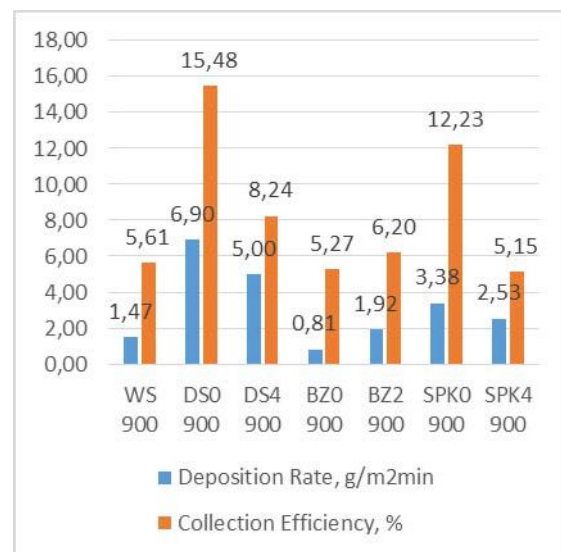
No.		WS	DS0 900	DS4 900	BZ0 900	BZ2 900	SPK0 900	SPK4 900	BS 1200 1100	BSA 1200 1100	BW 1200	BWA 1200
Fuel (+Add) stream, kg/h	B	1.06	1.754	1.847	1.526	1.562	1.681	1.768	2.250	2.500	1.75	1.94
Additive stream, kg/h	Ba	0	0	0.074	0	0.0312	0	0.071	0	0.225	0	0.078
Supply air, m <sup>3</sup> /h	Vp	9.15	8.53	8.73	8.35	8.41	8.36	8.20	10.04	10.04	8.3	8.3
Thermal input, kW	Q <sub>th</sub>	7.0	7.0	7.0	7.0	7.0	7.0	7.0	9.0	9.0	7.0	7.0
Probe inflow surface area, m <sup>2</sup>	F <sub>probe</sub> *	0.0349	0.0349	0.0349	0.0349	0.0349	0.0349	0.0349	0.0047	0.0047	0.0047	0.0047
Ash+Add stream, kg/h	m <sub>ash</sub>	0.111	0.189	0.257	0.065	0.131	0.117	0.208	0.215	0.440	0.148	0.361
Ash mass flow density, kg/m <sup>2</sup> h	m <sub>Fash</sub>	1.570	2.675	3.642	0.920	1.854	1.66	2.949	6.84	14.00	4.696	11.486
Indicator, %/kW	CE/Q <sub>th</sub>	0.21	0.98	0.71	0.12	0.27	0.48	0.36	0.69241	2,201,47	3.70	3.41
Temp. of probe, °C	t <sub>probe</sub>	480	480	480	480	480	480	480	12001100	12001100	1200	1200
Temp. of reactor, °C	t <sub>reactor</sub>	900	900	900	900	900	900	900	12001100	12001100	1200	1200
Excess Air Ratio, -	λ	1.21	1.19	1.22	1.16	1.17	1.21	1.19	1.15	1.15	1.15	1.15
Unburnt Carbon in bottom ash, %	UBC	0.24	1.40	1.26	0.73	0.57	0.33	0.41	-	-	-	-

\*F<sub>probe</sub> for PFCC test is calculated as lateral surface of the air cooled deposition probe A<sub>DC</sub> of PFCC test = π x 0.3m x 0.037m = 0.0349 m<sup>2</sup>; for BTS test A<sub>DC</sub>= π x 0.2 x 0.015/2 = 0.0047 m<sup>2</sup>

- Ash deposition tests performed by SUT:

Experiments were carried out for the constant fuel thermal input Q<sub>th</sub>=7.0 kW at reactor inner shell temperature 900°C for DS0, DS4, SPK0, SPK4, BZ0, BZ2 and WS. Excess air ratio λ was maintained at level of 1.20 +/-0.03 and measured in the port P3 (see Figure 3). In all tests, the primary air was maintained to keep 30-35% of total combustion air. The deposition tests lasted for 120 min and after exposure the collected deposits were weighed to determine deposition rate and collection effectiveness (CE) using eq. 2.1 and 2.2. In all tests, the time of deposit probe exposure was τ=120 min.

The results presented in this paper are the extension of research initiated in ref. [19], [23]. The calculated deposition rates and collection efficiencies are compared with each other in Figure 8. For the tests BZ0, BZ2 the positive effect of halloysite was not achieved as reflected by the higher collection efficiency obtained (CE(BZ0)=5.27%; CE(BZ2)=6.20%). For other tests, namely SPK4 and DS4 the deposit collection efficiency decreased as result of the additive interaction. In case of SPK4 the CE reached the level comparable with coal test (WS).

**Figure 8:** Ash deposition rate and collection efficiencies for temperature of experiments: 900°C (SUT).

Regarding the CE/Qth indicator which relates deposit collection efficiency with thermal input of fuel. Biomasses doped with halloysite indicate decrease of this factor (see Table VI). Moreover, the collected deposits with halloysite were more powdery, had different physical structure and color. Ash deposits formed without halloysite additive were highly sintered and built complex ash agglomerates (see Figure 9 and 10) which could be more difficult to be removed from the tube banks by applying sootblowers in pf boilers



**Figure 9:** Ash deposit collected during DS0 900°C tests - close-up image, visible sintered ashes and agglomerates; PFCC reactor.



**Figure 10:** Ash deposit collected during DS4 900°C tests - close-up image, powdery deposit; PFCC reactor.

- Ash deposition tests performed by IFK-USTUTT:  
The collected high temperature deposits during BTS tests at 1200°C and 1100°C were much more fused and/or sintered compared to deposits obtained from the tests at 900°C in PFCC rig. Moreover, the effects of additive dosage on reducing the molten phase in deposits were here more visible (please see Figure 10 and 11). In general, due to increased ash loading during biomass combustion with additive, higher ash deposition rates were measured for BSA and BWA tests. However, as results of less fused deposits formed with the additive, the developed deposits may be more easily removed by soot-blowers.

Apart from the ash deposition rate, the ash collection efficiency is the main indicator of the additive impacts. Based on the results obtained, this indicator may show different tendencies strongly dependent on the

temperature range. At temperature of 1200°C for BSA, both the ash deposition rate and collection efficiency increased significantly as compared to the test without additive (BS 1200), showing a negative impact of the additive use. However, at 1100°C, the ash collection efficiency dropped from 22% to 13%, clearly indicating positive effects on reducing deposit built-up. In case of BW 1200 and BWA 1200 tests, the collection efficiency slightly decreased with the additive use whereas the ash deposition rate was more than doubled. Taking into account that the deposits developed with such a high rate BWA 1200 were less fused as BW 1200, it may still be easier removed by soot-blowers or gravity than highly fused BW 1200.

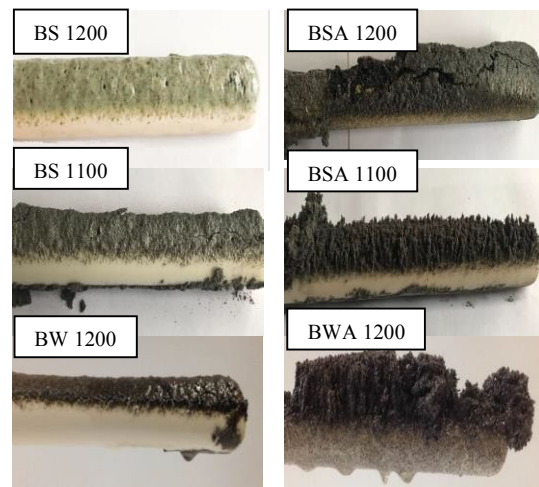


**Figure 11:** Pictures of the ash deposits collected on the ceramic probes during the BTS tests.



**Figure 12:** Ash deposition rate and collection efficiencies for temperature of experiments: 1100°C and 1200°C (USTUTT).

### 3.3 Ash oxides and AFT test of collected deposits

For the sake of fusibility tests of the collected ash, deposits were formed into pyramids. The maximal temperature of experiments did not exceed 1500°C under both the reduction reducing and oxidizing conditions. Initial deformation temperature (IDT), softening

temperature (ST), hemispherical temperature (HT), fluid temperature (FT) and its specific shapes were determined by camera and computer system according to the procedure and standards described in [29]. Results of ash fusibility experiments are shown in Table VII. Results of AFT tests confirmed that the addition of halloysite to biomass shifted the melting behavior of ash to coal ashes behavior. In reducing condition tests the shrinkage temperature for samples with addition of halloysite increased to BZ2=1130°C, SPK4=1020°C, DS4=1130°C compared to raw biomasses - BZ0=1050°C, SPK0=940°C, DS0=870°C respectively.

Major elements of ash (Al, Ca, Fe, Mg, P, K, Si, Na,

Ti, Mn, Sr) were determined using procedure [30] by Plasma Spectrometer Thermo iCAP 6500 Duo ICP. Chlorine content was determined by using the procedure described in [31]. Results of ash oxides analysis are presented in Table VIII. The increased content of Al<sub>2</sub>O<sub>3</sub> and Fe<sub>2</sub>O<sub>3</sub> for the additive doped biomass deposits indicates the presence of halloysite in the samples. The elevated chlorine content in the ashes from DS4 test (Cl=0.29%), as compared with DS0 (Cl=0.05%), indicates that under the same process condition chlorine could condensate on the cooled steel probe (probe shell temperature=480°C) even in the presence of halloysite.

**Table VII:** Results of ash fusibility experiments of investigated deposits.

Oxidizing Conditions									
Temp. °C/ Fuel	BZ0	BZ2	SPK0	SPK4	DS0	DS4	WS	BW	BWA
IDT	1110	1170	970	1110	1030	1150	1190	1170	1210
ST	1150	1240	1110	1180	1080	1190	1290	1260	n.a.
HT	1190	1280	1250	1260	1180	1240	1370	1280	1350
FT	1270	1290	1290	1300	1260	1290	1420	1350	1380

**Table VIII:** Results ash oxides analysis and chlorine content in investigated deposits.

Component. %/ Fuel	BZ0	BZ2	SPK0	SPK4	DS0	DS4	WS	BW	BWA
SiO <sub>2</sub>	52.97	42.42	56.21	51.44	62.00	51.71	57.94	56.5	49.0
Fe <sub>2</sub> O <sub>3</sub>	5.40	11.16	10.24	13.52	3.82	10.36	10.88	10.1	17.7
Al <sub>2</sub> O <sub>3</sub>	9.80	15.68	9.13	13.11	5.78	12.77	21.16	11.6	21.0
Mn <sub>3</sub> O <sub>4</sub>	0.19	0.38	0.28	0.35	0.13	0.29	0.05	0.305	0.430
TiO <sub>2</sub>	2.89	2.36	1.63	2.31	0.53	1.17	0.72	1.35	2.46
CaO	11.33	10.25	6.21	5.24	10.32	6.92	1.66	5.92	2.93
MgO	3.76	3.47	2.14	1.85	0.44	2.16	1.17	1.77	0.990
SO <sub>3</sub>	1.80	1.16	1.21	0.94	0.44	0.62	1.13	0.712	0.128
P <sub>2</sub> O <sub>5</sub>	2.74	2.83	2.24	2.04	3.01	2.14	0.18	1.87	1.28
Na <sub>2</sub> O	1.10	0.67	0.42	0.28	0.89	0.65	1.77	0.278	0.271
K <sub>2</sub> O	7.77	9.44	10.14	8.78	12.48	10.80	3.21	9.40	5.02
BaO	0.12	0.10	0.10	0.10	0.06	0.07	0.09	0.093	0.081
SrO	0.05	0.05	0.03	0.03	0.05	0.04	0.02	0.033	0.024
Cl	0.09	0.02	0.02	0.02	0.05	0.29	0.01	0.084	0.013

### 3.4 Deposit SEM-EDX analysis

After exposure tests, the ceramic probes with the collected ash deposits were initially embedded with epoxy resin to freeze further reactions and to avoid the loss of deposited material. Then, the samples were cut under dry conditions in the chop cutter using a diamond abrasive cutting wheel. Before performing the SEM/EDX analysis, the cross sections of the material samples were embedded again with resin and hardener. After embedding the samples were grinded and polished under dry condition. The example results from the SEM-EDX analysis of the two ash deposits collected during

combustion of straw with (BSA 1100) and without additive (BS 1100) at 1100°C conditions are shown in Figures 13-16.

The SEM-EDX images of the BSA 1100 deposit sample revealed apart from the less fused but extended sintered structure (as shown in Figures 15-16), a different composition of the deposit with the increased contents of alumina and iron elements originated from the additive.. Similarly as for BS 1100 deposits the calcium, potassium and silica oxides were present in BSA 1100 samples being the major ash forming elements derived from fuel. Elements originated from the additive, such as Al and Fe

were not uniformly distributed in deposit due to likely thermal decomposition of the additive. The higher content of alumina oxides from halloysite raised the melting temperature and affected the structure of the BSA 1100 deposit. Chlorine was found in very minor concentrations in some local spots of deposits. Based on

the phase equilibrium calculations [23] chlorine in the high temperature formed deposits is not supposed to be present either in solid or liquid phase, as opposed to the potassium which can form sticky or molten particles when reacted with (alumina)-silicates.

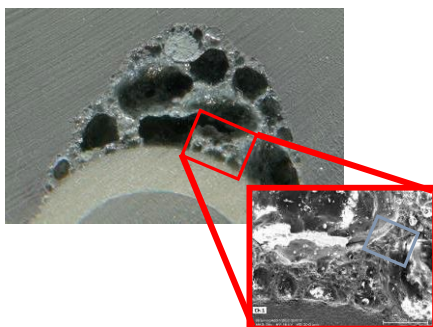


**Figure 13:** Microscopic picture and secondary electron image (SE) of the selected cut and area of the BS 1100 deposit sample for the SEM-EDX analysis

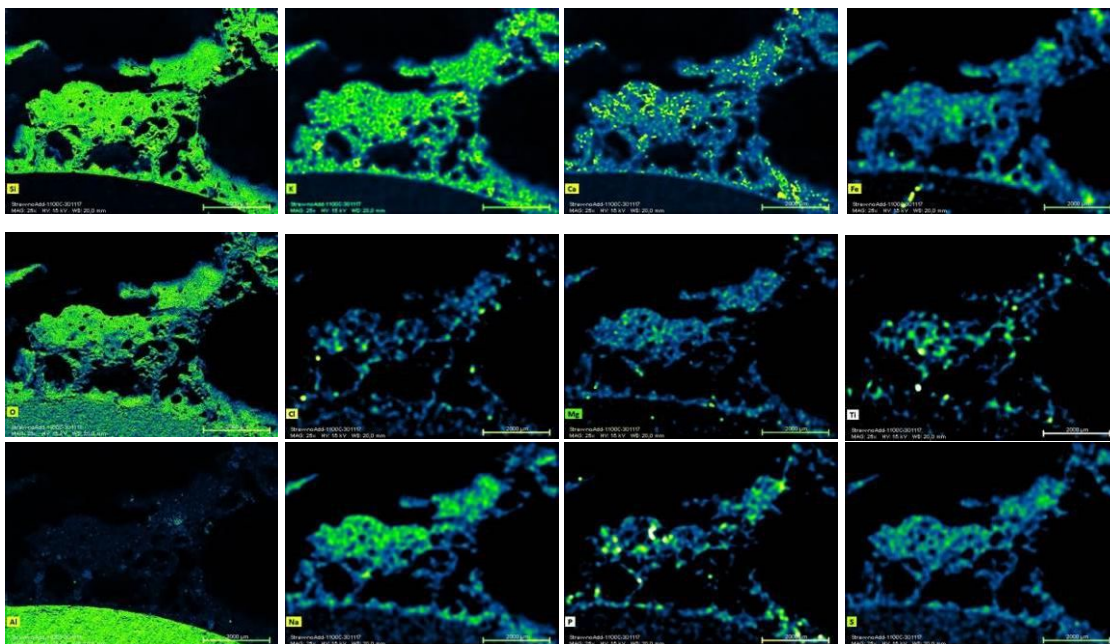


**Figure 14:** SEM-EDX mapping of the selected area of the BS 1100 deposit sample.

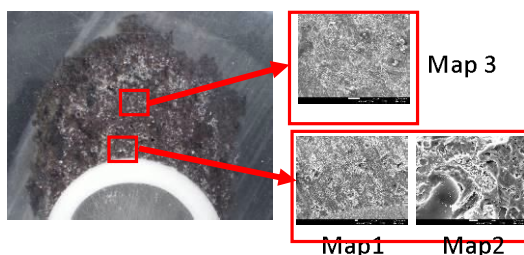


**Figure 15:** Microscopic picture and secondary electron images (SE) of the selected cut and areas of the BSA 1100 deposit sample for the SEM-EDX analysis.

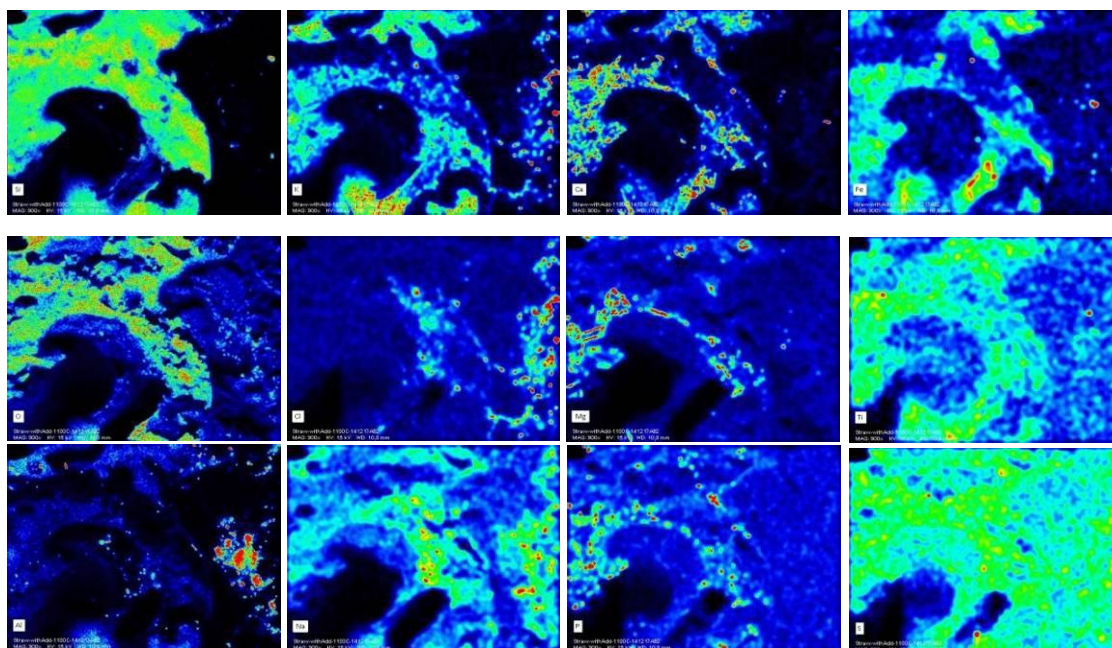


**Figure 16:** SEM-EDX mapping of the selected area (Map 2) of the BSA 1100 deposit sample.

#### 4 CONCLUSIONS

In this study the halloysite as an anti-slagging, anti-corrosion additive for biomass combustion in pulverized fuel fired systems has been investigated

The positive impact of halloysite on the ash deposit properties and potassium capture while reducing the chlorine content in corrosive deposits has been confirmed. However, the flue gas temperature of the formed deposits is a critical factor. The best effects of additive on reducing ash deposition rates and collection efficiencies when firing biomass have been observed in the flue gas temperature of 900°C. The decrease in the collection efficiency confirmed the effectiveness of the chosen dose of additive. Biomass ash deposits enriched with halloysite are more powdery and should be more easily removed by sootblowers. Their physical and chemical properties were closer to the ash deposits resulting from hard coal combustion. Although the use of additive reduced, in general, the chlorine content in deposits, the potassium remained in form of K-aluminosilicates.

The impact of halloysite on the ash deposits formed at temperature window of 1100°C-1200°C is more complex. Deposits formed with additive are less fused but have the extended sintered structure which may results in higher ash deposition and collection efficiencies. Therefore, for the furnace outlet temperatures above 1100°C, the use of halloysite as additive should be individually and carefully analyzed with the type of biomass planned to be fired.

The use of aluminosilicate based additives when firing biomass apart of its high effectiveness in potassium capture may in addition cause the increased HCl concentration in the flue gas.

#### 5 REFERENCES

- [1] Kalisz S., Ciukaj Sz., Mroczek K., Tymoszuik M., Wejkowski R., Pronobis M., Kubiczek H.; Full-scale study on halloysite fireside additive in 230 t/h pulverized coal utility boiler, *Energy*, Volume 92, Part 1 (2015) pages 33-39
- [2] Wang X., Liu Y., Tan H., Ma L., Xu T., Mechanism research on the development of ash deposits on the heating surface of biomass furnaces. *Ind Eng Chem Res* (2012) pages 12984–92.
- [3] Pronobis M; The influence of biomass co-combustion on boiler fouling and efficiency, *Fuel*, 85 (4) (2006), pages. 474-480
- [4] Chen M.Q., Yu D., Wei Y.H.: Evaluation on ash fusion behavior of eucalyptus bark/lignite blends, *Powder Technol.*, 286 (2015) pages 39-47
- [5] Tonn B., Thumm U., Lewandowski I., Claupein W, Leaching of biomass from semi-natural grasslands - effects on chemical composition and ash high-temperature behavior, *Biomass Bioenergy*, 36 (2012), pages 390-403
- [6] Niu Y., Zhu Y., Tan H., Wang X., Hui S.E., Du W.: Experimental study on the coexistent dual slagging in biomass-fired furnaces: alkali- and silicate melt-induced slagging, *Proc. Combust. Inst.*, 35 (2015), pages 2405-2413
- [7] Kassman H., Pettersson J., Steenari B.-M., Amand, Two strategies to reduce gaseous KCl and chlorine in deposits during biomass combustion - injection of ammonium sulphate and co-combustion with peat, *Fuel Process. Technol.*, 105 (2013), pp. 170-180
- [8] B. Wei, X. Wang, H. Tan, L. Zhang, Y. Wang, Z. Wang, Effect of silicon–aluminum additives on ash fusion and ash mineral conversion of Xinjiang high-sodium coal, *Fuel*, 181 (2016), pp. 1224-1229
- [9] Y. Ma, Z.Y. Huang, H.R. Tang, Z.H. Wang, J.H. Zhou, K.F. Cen, Mineral conversion of Zhundong

- coal during ashing process and the effect of mineral additives on its ash fusion characteristics, *J. Fuel Chem. Technol.*, 42 (1) (2014), pp. 20-25
- [10] Zevenhoven M., Yrja, P., Hupa M.: *Ash-Forming Matter and Ash-Related Problems. Handbook of Combustion*. Wiley-VCH Verlag GmbH & Co. KGaA. (2014) pages 3217-3223
- [11] Hardy T.: Use of aluminosilicate sorbents to control KCl vapors in biomass combustion gases, *Journal of Power Technologies* 93 (2013) pages 38-44
- [12] Wang G., Jensen P. A., Wu H., Jappe Frandsen F., Sander B., Glarborg P.: K-capture by Al-Si based Additives in an Entrained Flow Reactor. In *Impacts of Fuel Quality on Power Production* (2016)
- [13] Wang G., Jensen P. A., Wu H., Jappe Frandsen F., Sander B., Glarborg P.: Potassium Capture by Kaolin, Part 2: K<sub>2</sub>CO<sub>3</sub>, KCl, and K<sub>2</sub>SO<sub>4</sub>, *Energy and Fuels* 32 (2018) pages 3566-3578
- [14] Wang G., Jensen P. A., Wu H., Jappe Frandsen F., S Laxminarayanander Y., B., Glarborg P.: KOH capture by coal fly ash, *Fuel*, 242 (2019) pages 828-836
- [15] Raask E.: *Mineral impurities in coal combustion : behaviour, problems, and remedial measures*. Washington; London: Hemisphere (1985)
- [16] Kalisz S., Ciukaj Sz., Mroczek K., Kress T., Tymoszek M., Wejkowski R., Pronobis M., Kubiczek H. Impact of halloysite fuel additive on 650 t/h PC boiler co-firing biomass. Part I - deposition characteristics. 12th International Conference on Boiler Technology 2014.
- [17] Kress T., Maj I., Pronobis M., Kalisz S., Wejkowski R. Fuel additive influence on the fouling process while burning 100% biomass in experimental combustion chamber. 12th International Conference on Boiler Technology 2014.
- [18] Mroczek K., Kalisz S., Tymoszek M., Pronobis M., Sołtys J., Warchoń S. Full-scale study on application of halloysite additive in a hybrid installation co-firing high shares of agricultural biomass with pulverized coal. part II – mineral matter characteristics. 12th International Conference on Boiler Technology 2014.
- [19] Gądek W., Ciukaj S., Kalisz S.: Combustion characteristic of halloysite doped biomass: Impact on ash deposition tendency. *Contemporary problems of power engineering and environmental protection 2018. Circular economy*. Ed. by Krzysztof Pikoń and Magdalena Bogacka. Gliwice : Department of Technologies and Installations for Waste Management. Silesian University of Technology (2019) pages 53-61
- [20] Niu Y., Tan H., Hui S., Ash-related issues during biomass combustion: Alkali-induced slagging, silicate melt-induced slagging (ash fusion), agglomeration, corrosion, ash utilization, and related countermeasures, *Progress in Energy and Combustion Science* 52 (2016) pages 1-61.
- [21] Bostrom D., Skoglund N., Grimm A., Boman C., Ohman M., Brostrom M., Backman R., Ash transformation chemistry during combustion of biomass. *Energ Fuel* (2012) pages 85-93.
- [22] Lindberg D., Backman R., Chartrand P., Hupa M., Towards a comprehensive thermodynamic database for ash-forming elements in biomass and waste combustion—Current situation and future developments. *Fuel Process Technol.* 105 (2013) pages 129-41.
- [23] Płaza P., Maier J., Maj I., Gądek W., Kalisz S.: Potassium and chlorine distributions in hightemperature halloysite formed deposits. *E3S Web of Conferences* 82 (2019), ICBT Poland 2018
- [24] Barroso J., Ballester J., Ferrer L. M., Jimenez S.: Study of coal ash deposition in an entrained flow reactor: Influence of coal type, blend composition and operating conditions. *Fuel Processing Technology* 87 (2006) pages 737 – 752.
- [25] Wandrasz J., Wandrasz A.: *Paliwa Formowane*. Wydawnictwo Seidel-Przywecki Sp. z o.o. Warszawa 2006.
- [26] Weber R., Kupka T., Zajac K.: Jet flames of refuse derived fuel. *Combustion and Flame* 156 (2009) pages 922 – 927.
- [27] Ndibe C., Maier J., Scheffknecht G.: Combustion, cofiring and emissions characteristics of torrefied biomass in a drop tube reactor. *Biomass & Bioenergy* 79 (2015) pages 105 - 115.
- [28] Weber R., Y. Poyraz, A. M. Beckmann, S. Brinker.: Combustion of biomass in jet flames. *Proceedings of the Combustion Institute* 35. (2015) pages 2749 – 2758.
- [29] PN-ISO 540:2001: Paliwa stałe - Oznaczenie topliwości popiołu w wysokiej temperaturze metodą rurową.
- [30] PN-EN ISO 16967:2015-06: Biopaliwa stałe - Oznaczenie pierwiastków głównych - Al, Ca, Fe, Mg, P, K, Si, Na i Ti. (2015).
- [31] PN-EN 196-2:2013-11: Metody badania cementu - Część 2: Analiza chemiczna cementu.
- [32] Mikunda W. : Biomass valorization through additive dosage. Master thesis realized in the frame of Erasmus EU Student exchange programme between SUT and USTUTT. 2017.
- [33] Paneru M. et al. Characterization of deposition behaviour of various fuel/fuel-additive mix using online deposition measurement sensor. *Proceedings of the 27<sup>th</sup> Conference on Impacts of Fuel Quality on Power Production*, Lake Louise, Canada, 2018.

## 6 ACKNOWLEDGMENT

The research presented in this paper was performed within projects: “Advanced pretreatment and characterization of Biomass for Efficient Generation of heat and power” (BioEffGen) funded by the National Centre for Research and Development in Poland and the Federal Ministry of Education and Research in Germany within Polish-German Sustainability Research Programme (STAIR) and “Process optimisation and valorisation of combustion by-products in transition to circular economy” (UPS-Plus) funded by The Foundation for Polish Science within Team Teach Core Facility Programme.

The SEM-EDX analysis of the deposit samples were carried out by Eva Miller from IFK (USTUTT). Part of the ash deposition tests planned at IFK (USTUTT) were performed by Wojciech Mikunda in the frame of Erasmus EU Student exchange programme between SUT and USTUTT.